Zweitveröffentlichung/
Secondary Publication

Staats- und
Universitätsbibliothek
Bremen

https://media.suub.uni-bremen.de

Wolfgang Dreher, Ingo Bardenhagen, Li Huang, Marcus Bäumer

On the suppression of background signals originating from NMR hardware components. Application to zero echo time imaging and relaxation time analysis

Journal Article as: peer-reviewed accepted version (Postprint)

DOI of this document*(secondary publication): https://doi.org/10.26092/elib/2469

Publication date of this document: 08/09/2023

* for better findability or for reliable citation

Recommended Citation (primary publication/Version of Record) incl. DOI:

Wolfgang Dreher, Ingo Bardenhagen, Li Huang, Marcus Bäumer, On the suppression of background signals originating from NMR hardware components. Application to zero echo time imaging and relaxation time analysis, Magnetic Resonance Imaging,Volume 34, Issue 3,2016,Pages 264-270,ISSN 0730-725X,https://doi.org/10.1016/j.mri.2015.10.008.

Please note that the version of this document may differ from the final published version (Version of Record/primary publication) in terms of copy-editing, pagination, publication date and DOI. Please cite the version that you actually used. Before citing, you are also advised to check the publisher's website for any subsequent corrections or retractions (see also https://retractionwatch.com/).

This document is made available under a Creative Commons licence.

The license information is available online: https://creativecommons.org/licenses/by-nc-nd/4.0/

Take down policy

If you believe that this document or any material on this site infringes copyright, please contact publizieren@suub.uni-bremen.de with full details and we will remove access to the material.

Technical note

On the suppression of background signals originating from NMR hardware components. Application to zero echo time imaging and relaxation time analysis

Wolfgang Dreher [a,*], Ingo Bardenhagen [b], Li Huang [a], Marcus Bäumer [b]

[a] University of Bremen, Department Chemistry, in-vivo-MR group, Bremen, Germany
[b] University of Bremen, Department Chemistry, Institute of Applied and Physical Chemistry, Bremen, Germany

ARTICLE INFO

Article history:
Received 9 February 2015
Revised 15 October 2015
Accepted 17 October 2015

Keywords:
Zero echo time (ZTE)
Relaxation time analysis
T_1 relaxation
Outer volume suppression (OVS)
Higher-order shim coils
Porous media

ABSTRACT

Modern NMR imaging systems used for biomedical research are equipped with B_0 gradient systems with strong maximum gradient strength and short switching time enabling ^{1}H NMR measurements of samples with very short transverse relaxation times. However, background signal originating from non-optimized RF coils may hamper experiments with ultrashort delays between RF excitation and signal reception. We demonstrate that two simple means, outer volume suppression and the use of shaped B_0 fields produced by higher-order shim coils, allow a considerable suppression of disturbing background signals. Thus, the quality of NMR images acquired at ultrashort or zero echo time is improved and systematic errors in quantitative data evaluation are avoided. Fields of application comprise MRI with ultrashort echo time or relaxation time analysis, for both biomedical research and characterizing porous media filled with liquids or gases.

1. Introduction

Recently, the performance of NMR imaging systems dedicated to preclinical NMR imaging and localized *in vivo* NMR spectroscopy has been improved considerably, particularly regarding the maximum strength and the slew rate of B_0 gradients. Therefore, these systems also allow applying various NMR methods with ultrashort echo times, e.g., to characterize porous materials despite inherently short transverse relaxation times. However, while the manufacturers provide some appropriate pulse sequences, problems may arise if standard radiofrequency (RF) coils are used, which are not proton-free [1]. Thus a simple pulse-acquire experiment performed without any sample will yield a considerable signal originating from support material or electronic components of the RF coil. These "background" signals can be neglected for most biomedical measurements as they decay within the first 300–500 μs after RF excitation. However, they will cause severe errors and artifacts when performing experiments with a very short delay between RF excitation and data acquisition, such as MRI with ultrashort echo time (UTE) or zero echo time (ZTE) [2–5]. This may affect *in vivo* measurements and will often hamper non-biomedical applications such as studies on the distribution and properties of liquids or gases in porous media due to the inherently very short effective transverse relaxation time T_2^* [6].

In the following, we describe how this problem of unwanted background signals can be solved by two simple means. While outer volume suppression (OVS) RF pulses [7–9] may considerably suppress the background signals, remaining contributions can be further reduced by the shaped B_0 fields produced by higher-order shim coils [10], particularly for smaller samples positioned in the center of the RF coil. Thus, dependent on the sample measured and the pulse sequence used, an adequate suppression of disturbing background signals can be achieved. Results from ZTE imaging experiments and T_1 relaxation time measurements [11–15] demonstrate the efficacy of these simple approaches, which should be applicable on most preclinical or clinical NMR systems.

2. Materials and method

2.1. Hardware

All experiments were performed on a preclinical MRI scanner BioSpec 70/20 USR (Bruker Biospin MRI GmbH, Ettlingen, Germany)

* Corresponding author at: Universität Bremen, Fachbereich 2 (Chemie), AG in-vivo-MR, Leobener Str., NW2-C, D-28359 Bremen, Germany. Tel.: +49 421 21863090; fax: +49 421 21863101.
E-mail address: wdreher@uni-bremen.de (W. Dreher).

operating at 7.05 T and being equipped with a standard gradient set BGA12S2 (maximum gradient strength 441 mT/m, rise time 130 μs). A commercial quadrature Birdcage coil (Bruker MRI GmbH, Ettlingen, Germany; 72 mm inner diameter, 112 mm outer diameter, "MT0100") was used for both RF excitation and reception of ^{1}H NMR signals. Pulse sequence modifications were performed on the ACQP level of the Paravision 5.1 software platform using Tcl/Tk shells for setting sequence parameters. Measurements were performed either without a sample to evaluate the background signals originating from the hardware or with a sample placed on a sample holder made of proton-free Teflon.

A piece of rubber and a highly porous monolithic carbon xerogel filled with dimethyl sulfoxide (DMSO) (for details see [15]) were used as samples for ZTE imaging and T_1 measurements, respectively.

2.2. Outer volume suppression (OVS)

To suppress background signals originating from the RF coil, we inserted OVS pulses, i.e. a series of spatially selective RF pulses into the pulse sequences applied for ZTE imaging and T_1 measurements. This suppression module consisted of a series of sech-shaped RF pulses (duration 614.4 or 819.2 μs), followed by spoiler gradients to destroy transverse magnetization, which were applied immediately prior to RF excitation. The OVS pulses were applied prior to each excitation pulse of the ZTE MRI sequence or each scan of the T_1 measurements. The slice thickness (40 mm), the central position (±40–45 mm) and the values of the RF transmitter power expressed by the flip angle (30°–90°) were empirically optimized for the different measurements.

The aim of this optimization was to find a compromise between suppressing background signals and avoiding signal losses from the sample, which is easier for a distinct spatial separation between the sample and the sources of the background signals, i.e. small samples positioned in the center of the RF coil. Note that the values for the flip angle and the slice thickness are rather nominal values because the OVS pulses are applied beyond the spatial region exhibiting a homogeneous B_1 field and a constant B_0 gradient.

2.3. Use of higher-order shims

Shaped B_0 fields produced continuously by higher-order shim coils were used to suppress remaining background signals, particularly those originating from the cylindrical support material of the RF coil. The B_0 field of higher-order shim coils will cause stronger dephasing in the periphery, where the sources of the background signals are located. The influence of shaped B_0 fields of the yz- and xz-shim coils was estimated by a simple simulation program written in Scilab 5.5.1 (free and open source software, Scilab Enterprises, available from: http://www.scilab.org) showing that a considerable suppression of these background signals can be achieved. Thus, the signal decay originating from a cylinder was calculated (diameter 73 mm, length 80 mm corresponding to the sensitive volume of the used RF coil) by adding the signal contributions from a mash with 100×360 points in cylindrical coordinates. For comparison, the signal was calculated for a $20 \times 20 \times 20$ mm^3 cube mimicking a homogeneous sample in the center of the magnet. Fig. 1 displays the time domain signal for three different values of the yz- and xz-shim currents, given in percent of the maximum shim current of 3 A corresponding to 2016 Hz/cm^2 for the yz-shim and 2127 Hz/cm^2 for the xz-shim. All signals are plotted in percent of the maximum value after RF excitation.

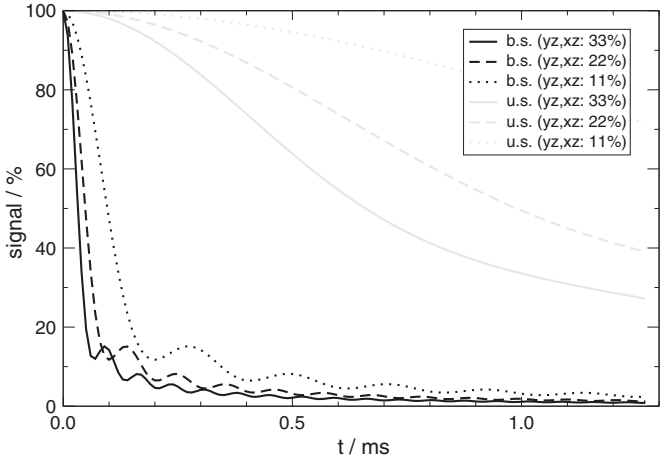

Fig. 1. Simulated time domain signals for the background signal ("b.s.") and the used sample signal ("u.s.") using different values of the yz- and xz-shim currents (in percent of maximum values). A cylinder and a cube were used as simple models for simulating the background signal and the sample signal, respectively (cf., Materials and methods).

2.4. Pulse-acquire experiments

To evaluate the disturbing background signals, pulse-acquire experiments were performed without or with OVS pulses and with or without applying higher-order shim currents. As in the pulse sequence used for T_1 measurements, RF excitation was performed by a 32 μs rectangular pulse and data acquisition started 50 μs after the center of the RF pulse.

2.5. Pulse sequence for ZTE imaging

The ZTE pulse sequence provided with Paravision 5.1 was used without or with inserted OVS pulses as described above. The read gradient was switched on 1.2 ms prior to the excitation pulse to avoid any effects of eddy currents, and switched off after data acquisition to reduce the gradient duty cycle. The sequence parameters were as follows: receiver bandwidth 100 kHz with 8-fold oversampling, repetition time TR of 7.5 ms or 9.1 ms if two (in y direction) or four (in x and y direction) OVS pulses were used, respectively; 2 μs 5° rectangular excitation pulse, FOV: $51.2 \times 51.2 \times 51.2$ mm^3, $128 \times 128 \times 128$ image matrix, one average per k-space spoke.

2.6. Pulse sequence for T_1 measurements

Partial saturation experiments [16] were performed for T_1 measurements by using a 32 μs 90° rectangular pulse for RF excitation and starting data acquisition 50 μs after the center of the RF pulse. The delay of 50 μs was chosen to ensure an almost complete suppression of background signals if both means of suppressing background signals (OVS and shape B0 fields by higher-order shims) were applied. In a series of 72 measurements, each with four averages preceded by four dummy cycles, the repetition time was reduced from 7 s to 25 ms. Considering a typical line width (full width at half maximum) of about 500 Hz for the DMSO signal in the xerogel, 512 complex data points were acquired with a spectral width of 100 kHz.

2.7. Data processing

While ZTE images were reconstructed on the console using Paravision 5.1, the pulse-acquire and the T_1 measurements were evaluated by in-house developed programs written in the interactive data language IDL (version 7.0, Exilis Visual Information Solutions,

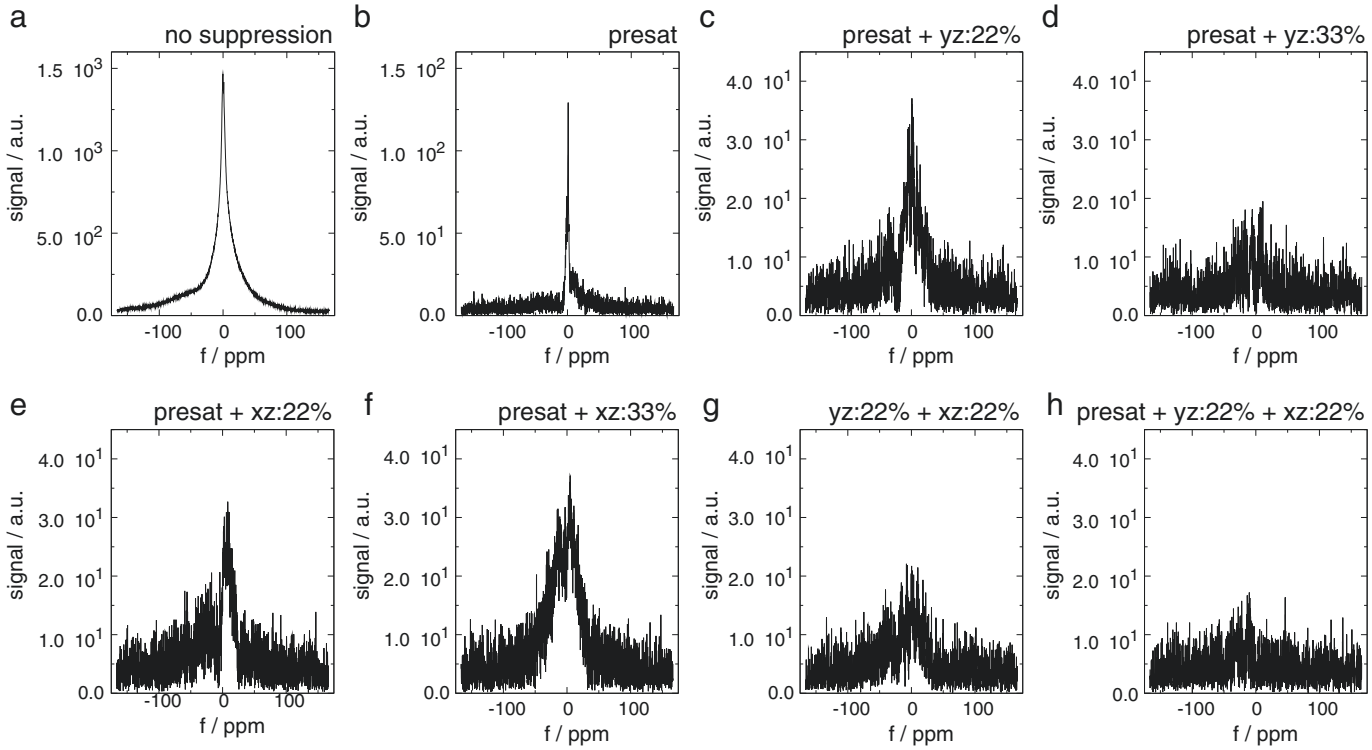

Fig. 2. Magnitude spectra of the background signal measured without inserting a sample into the RF coil. Measurements were performed with or without presaturation and with or without additional magnetic fields from yz- and/or xz-shim (in percent of maximum shim currents). (a) without presaturation and without yz- or xz-shim, (b) with presaturation, (c) with presaturation and yz-shim: 22%, (d) with presaturation and yz-shim: 33%, (e) with presaturation and xz-shim: 22%, (f) with presaturation and xz-shim: 33%, (g) with yz- and xz-shim: 22 %, (h) with presaturation and yz- and xz-shim: 22 %. Note the different scaling of spectra (a), (b) and (c–h).

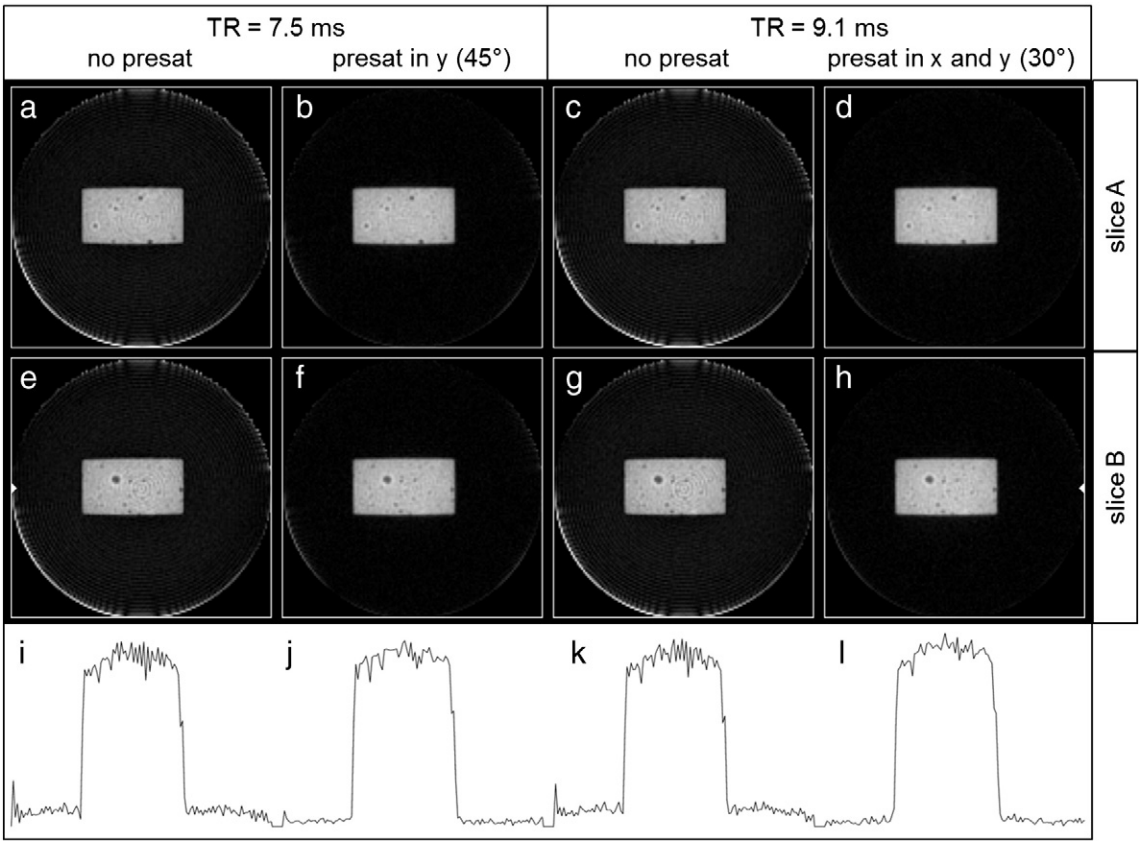

Fig. 3. ZTE images of a rubber phantom measured without or with additional presaturation pulses. Images (a–d) and (e–h) originate from two different slices of the 3D images and are displayed with the same absolute scaling. (a, e) without presaturation, TR = 7.5 ms; (b, f) with presaturation in y-direction and nominal flip angle of 45°, TR = 7.5 ms; (c, g) without presaturation, TR = 9.1 ms; (d, h) with presaturation in x- and y-direction and nominal flip angle of 30°, TR = 9.1 ms. (i–l) profiles through the images (e–h) of slice B at a position indicated by white arrows.

Bolder, USA). After Fourier transformation, the spectra were evaluated in the magnitude mode. For T_1 measurements by a series of partial saturation measurements, the signal intensity was determined for all TR values by peak area integration (±5 kHz). Mono- or biexponential fitting was performed using a Levenberg–Marquardt algorithm (LMFIT).

3. Results

Fig. 2 displays magnitude spectra of the background signals measured by a pulse-acquire experiment without inserting a sample into the RF coil. Although the strong background signal measured without any suppression (spectrum a), is not a single Lorentzian, a monoexponetial fit of the FID was performed by the matrix pencil method yielding 140 µs as a typical decay constant. The strong background signal can be suppressed by applying slice-selective presaturation RF pulses and/or additional magnetic fields from yz- and/or xz-shim coils (strength in % of maximum shim current). While only presaturation pulses were used for spectrum (b), 22% or 33% of the maximum yz- or xz-shim currents were additionally applied for spectra (c)–(f). The background signal can be suppressed almost to the noise level by using both higher-order shim coils simultaneously (spectrum g), particularly when combining the effects of higher-order shims with slice-selective presaturation (spectrum h).

Fig. 3 displays images from two slices (a–d, e–h) of 3D ZTE images, demonstrating the importance of suppressing background signals. While images (a, e) and (c, g) were measured without any suppression of background signals, images (b, f) and (d, h) were measured with presaturation in y-direction, and both y- and x-direction, respectively. The repetition time TR was 7.5 ms (a, b, e, f) or 9.1 ms (c, d, g, h) because of the different duration required for presaturation in one or two directions. The ring-shaped artifacts observed in the center of all images measured without suppression of background signals disappear if background signals are suppressed, particularly if presaturation is applied in both x- and y-direction. Additionally, reconstruction artifact signals, occurring as strong signals at the edges of the inner circle of the FOV are reduced. The reduced ringing artifacts and the flattened baseline are also visible in the equally scaled profiles (i–l) which correspond to images (e–h).

Fig. 4 shows the results of partial saturation experiments performed (a, b) on a xerogel filled with DMSO, and (c, d) performed without a sample. Both spatially selective presaturation and high values of yz- and xz-shim currents were used to suppress background signals for data in Fig. 4a and c, while the peak area values displayed in Fig. 4b and d versus the repetition time TR were measured without suppressing background signals. Comparing subfigures (a), (b) and (d), particularly for longer TR values, shows that the background signals contribute considerably by adding more than 25 % to the signal originating from the DMSO signal in the xerogel. Thus an efficient suppression of background signals is indeed required if the estimated T_1 values are to be used to characterize the liquid–surface interaction in the xerogel and systematic studies on T_1 changes with varying filling state are to be performed [15]. Fig. 4c demonstrates the suppression of the background signal by the combined use of spatially selective presaturation and higher-order shims. The background signal was

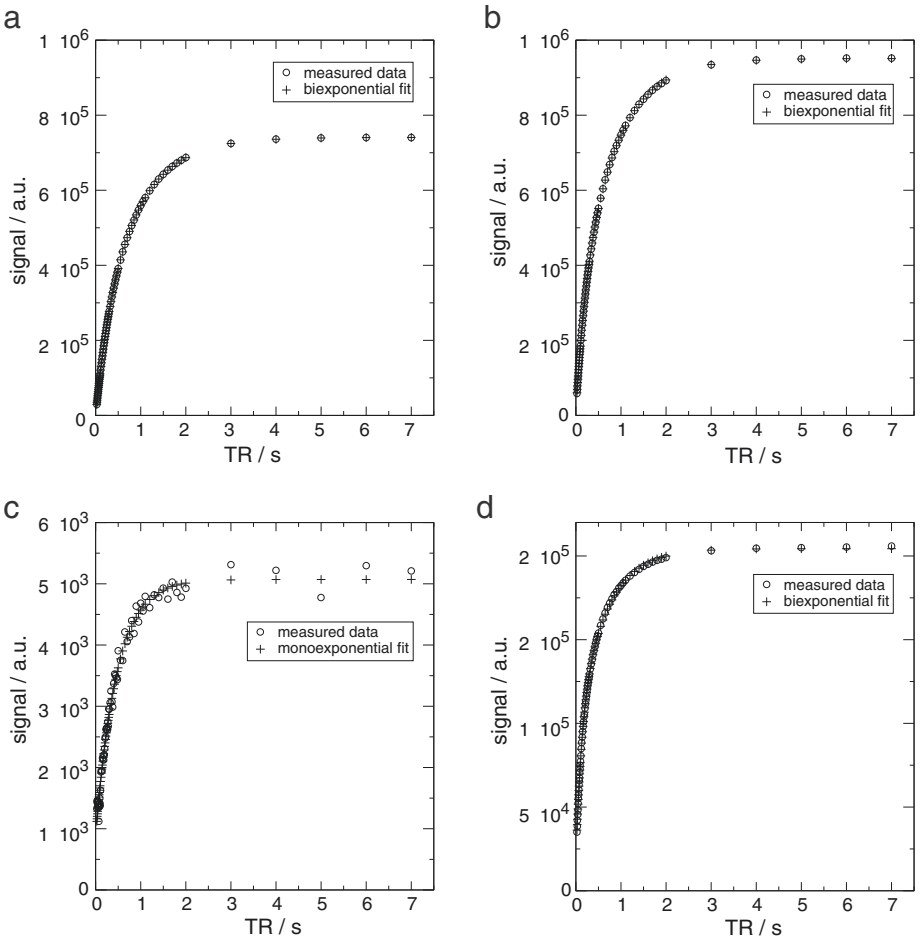

Fig. 4. Peak areas determined from magnitude spectra of partial saturation experiments with 72 different repetition times performed (a, b) on a xerogel filled with DMSO, or (c, d) without a sample. (a, c) With presaturation and additional yz- and xz-shim currents of 33%, (b, d) without presaturation or additional yz- and xz-shim currents.

efficiently suppressed by more than a factor of 40, corresponding to less than 1% of the DMSO signal from the xerogel. A biexponential fit yielded only one relevant component, i.e. the remaining background signals could be fitted by a monoexponential function.

It is noteworthy that excellent biexponential fitting is possible for the DMSO data measured with or without suppression of background signals (cf. Fig. 4a and b). Table 1 shows that the amplitudes and the T_1 relaxation times determined by biexponential fitting are significantly different between measurements performed without or with suppression of background signals. The relaxation times and the ratio between the amplitudes of the two components (A(long T_1)/A(short T_1)) are underestimated if the background signals are not adequately suppressed. Thus an insufficient suppression of background signals will cause systematic errors in the estimated parameters, resulting in potential misinterpretation of T_1 measurements.

4. Discusssion

Whereas a proton-free sample holder (e.g. made of Teflon) may rather easily be obtained, background signals originating from support material or electronic components of the RF coil may cause considerable problems for NMR measurements that use ultrashort or zero echo time data acquisition. Of course, the best experimental approach would be to use RF coils that are optimized with respect to background signals, thus avoiding or minimizing background signals being superimposed on the sample signal. However, we demonstrate that these disturbing background signals can be efficiently suppressed by using spatially selective outer volume suppression pulses and/or exploiting signal dephasing caused by spatially inhomogeneous B_0 fields due to higher-order shim coils. Thus, NMR imaging with ultrashort echo times or relaxation time measurements can be performed for characterizing porous samples, even with standard RF coils, which are routinely used for biomedical application.

The specific parameters of slice selective presaturation pulses (pulse shape, duration, RF power), their number and spatial orientation as well as their temporal order have to be determined as a compromise between suppression efficacy and potential disadvantages. While OVS pulses can be inserted in most pulse sequences, drawbacks of this approach comprise (i) a prolonged minimum repetition time and thus a longer minimum total measurement time, (ii) increased RF power deposition which may lead to increased temperature of the sample, (iii) potential signal losses from the sample due to partial saturation or magnetization transfer effect due to off-resonance preirradiation [17], and (iv) reduced suppression efficacy for background signals with ultrashort T_2^*. Considering the latter drawback, the pulse duration of the OVS pulses should be as short as possible. Additionally, using OVS pulses for ZTE MRI means that this pulse sequence loses one of its attractive features for biomedical applications because it cannot be applied as a silent MRI sequence. However, this additional disadvantage is of limited importance for applications to material sciences.

Table 1
Amplitudes and T_1 relaxation times estimated by (a, b, d) biexponentially or (c) monoexponentially fitting the data measured on a xerogel filled with DMSO (cf., Fig. 4).

Measurements	A_a/a.u.	$T_{1,a}$/ms	A_b/a.u.	$T_{1,b}$/ms
a. with sample, with suppression of background signals	$5.85 \cdot 10^5$ (±0.3%)	837 (±0.2%)	$1.57 \cdot 10^5$ (±1.1%)	285 (±0.7%)
b. with sample, without suppression of background signals	$7.21 \cdot 10^5$ (±1.5%)	788 (±0.5%)	$2.19 \cdot 10^5$ (±4.4%)	197 (±1.6%)
c. without sample, with suppression of background signals	$4.17 \cdot 10^3$ (±1.4%)	472 (±3.8%)	–	–
d. without sample, without suppression of background signals	$1.10 \cdot 10^5$ (±1.5%)	624 (±1.7%)	$7.65 \cdot 10^4$ (±2.0%)	125 (±2.7%)

The errors were given by the fitting routine.

Currently, the use of dual-band RF pulses is considered to reduce the total duration of the OVS module [18–20]. Another option may be to use OVS pulses only after every n-th ($n > 1$) ZTE acquisition, similar to the ZTE method with suppressed long T_2 components proposed by Weiger et al. [21]. This modification would reduce time losses caused by OVS pulses and the subsequent spoiler gradients, although at the expense of the suppression efficacy. In general, one should emphasize that an empirical optimization of the presaturation module is necessary because the suppression of background signals is performed in a spatial range of low B_0 and B_1 homogeneity, where also the magnetic field produced by the gradient coils is highly nonlinear. Finally, the OVS approach cannot suppress background signals originating from regions where the B_0 field produced by the gradient coil is no longer monotonic. However, for most hardware configurations (RF coil, B_0 gradient), the sensitivity of RF coil will also decrease for these background signals.

The suppression of background signals by using shaped B_0 fields of higher-order shim coils is, of course, easy to achieve as it is not necessary to modify pulse sequences. However, the added inhomogeneity of the static magnetic field will also cause a faster decay of the sample signal. Thus, the signal-to-noise ratio (SNR) will be reduced and the corresponding line broadening will decrease the spatial resolution of MRI experiment. However, for smaller samples, i.e., low filling factor of the RF coil, these disadvantages are often acceptable, as demonstrated by the two examples (cf., Figs. 3 and 4). The B_0 field produced by the higher-order shim coils varies slowly in the magnet center, where the sample is located, but more strongly further outside, where the background signals are to be suppressed.

The strength of the applied higher-order shim currents has to be chosen as a compromise between the desired suppression of the background signals and the unwanted line broadening and SNR reduction. If used for ZTE MRI, stronger higher-order shim currents are required for a comparable suppression of background signals, when a higher readout bandwidth is used corresponding to a reduced acquisition period. The selection of shim coils used for efficiently suppressing background signals will depend on the available shims coils. However, the use of "mixed terms" (such as yz- or xz-shim coils used in this study) is certainly a good choice to suppress signals from rather homogeneously distributed signal sources such as the proton containing support material of an RF coil. Currently our MR system exhibits only five second-order shim coils. However, if available, the use of shims of higher than second order may improve the suppression efficacy.

Finally, while higher-order shim coils allow for an efficient suppression of background signals from the (cylindrical) support material of the coil, this approach is not adequate for suppressing background signals from well-localized sources such as capacitors or diodes. Signals from such electronic components can be better suppressed by OVS RF pulses.

For ZTE, other methods for suppressing background signals have been proposed by Weiger et al., e.g. by exploiting T_2 differences [22] or subtracting data acquired without the sample from data measured with the sample [23]. These methods as well as the two approaches described above have their specific advantages and drawbacks. For instance, while the subtraction approach [22] avoids prolonged TR values and requires a rather large FOV, the OVS approach can be used with a small FOV and does not require a reference scan without sample but with adjusted coil loading. Thus, which suppression method or which combination of these methods is the best choice depends on the sample and the sequence parameters used.

5. Conclusion

We have demonstrated that unwanted background signals originating from the support material and/or electronic components of the RF coil can be efficiently suppressed by using outer volume suppression RF pulses and/or signal dephasing due to the shaped B_0 fields caused by higher-order shim coils. If only non-optimized hardware components are available such as standard RF coils routinely used on a preclinical or clinical MR imaging system, these two means for suppressing background signals allow improved data quality for experiments with a very short delay between RF excitation and data acquisition. Thus, it is possible to avoid or at least reduce artifacts in MR images acquired with ultrashort or zero echo time as well as systematic errors in quantitative studies such as relaxation time measurements.

Acknowledgment

This work was in part supported by the German Research Foundation (DFG) within the Research Training Group GRK 1860 "Micro-, meso- and macroporous nonmetallic Materials: Fundamentals and Applications" (MIMENIMA).

References

[1] Horch RA, Wilkens K, Gochberg DF, Does MD. RF coil considerations for short-T_2 MRI. Magn Reson Med 2010;64:1652–7.
[2] Robson MD, Gatehouse PD, Bydder M, Bydder GM. Magnetic resonance: an introduction to ultrashort TE (UTE) imaging. J Comput Assist Tomogr 2003;27:825–46.
[3] Gatehouse PD, Bydder GM. Magnetic resonance imaging of short T_2 components in tissue. Clin Radiol 2003;58:1–19.
[4] Tyler DJ, Robson MD, Henkelman RM, Young IR, Bydder GM. Magnetic resonance imaging with ultrashort TE (UTE) pulse sequences: technical considerations. J Magn Reson Imaging 2007;25:279–89.
[5] Weiger M, Pruessmann KP, Hennel F. MRI with zero echo time: hard versus sweep pulse excitation. Magn Reson Med 2011;66:379–89.
[6] Watson AT, Chang CP. Characterizing porous media with NMR methods. Progr NMR Spectr 1997;31:343–86.
[7] Singh S, Rutt BK, Henkelman RM. Projection presaturation: a fast and accurate technique for multidimensional spatial localization. J Magn Reson 1990;87:567–83.
[8] Duyn JH, Gillen J, Sobering G, van Zijl PC, Moonen CT. Multisection proton MR spectroscopic imaging of the brain. Radiology 1993;188:277–82.
[9] Luo Y, de Graaf RA, DelaBarre L, Tannús A, Garwood M. BISTRO: an outer-volume suppression method that tolerates RF field inhomogeneity. Magn Reson Med 2001;45:1095–102.
[10] Koch KM, Rothman DL, de Graaf RA. Optimization of static magnetic field homogeneity in the human and animal brain in vivo. Progr NMR Spectr 2009;54:69–96.
[11] Brownstein K, Tarr C. Spin-lattice relaxation in a system governed by diffusion. J Magn Reson 1977;26:17–24.
[12] Borgia GC, Fantazzini P, Mesini E. Water ^{1}H spin-lattice relaxation as a fingerprint of porous media. Magn Reson Imaging 1990;8:435–47.

[13] Chen S, Liaw HK, Watson AT. Fluid saturation dependent nuclear magnetic resonance spin lattice relaxation in porous media and pore structure analysis. J Appl Phys 1993;74:1473–9.
[14] Simina M, Nechifor R, Ardelean I. Saturation-dependent nuclear magnetic resonance relaxation of fluids confined inside porous media with micrometer-sized pores. Magn Reson Chem 2011;49:314–9.
[15] Bardenhagen I, Dreher W, Fenske D, Wittstock A, Bäumer M. Fluid distribution and pore wettability of monolithic carbon xerogels measured by ^{1}H NMR relaxation. Carbon 2014;68:542–52.
[16] Freeman R, Hill H. Fourier transform study of NMR spin–lattice relaxation by "progressive saturation". J Chem Phys 1971;54:3367–77.
[17] Henkelman RM, Stanisz GJ, Graham SJ. Magnetization transfer in MRI: a review. NMR Biomed 2001;14:57–64.
[18] Smith MA, Gillen J, McMahon MT, Barker PB, Golay X. Simultaneous water and lipid suppression for in vivo brain spectroscopy in humans. Magn Reson Med 2005;54:691–6.
[19] Gu M, Spielman DM. B_1 and T_1 insensitive water and lipid suppression using optimized multiple frequency-selective preparation pulses for whole-brain ^{1}H spectroscopic imaging at 3T. Magn Reson Med 2009;61:462–6.
[20] Zhu H, Ouwerkerk R, Barker PB. Dual-band water and lipid suppression for MR spectroscopic imaging at 3 Tesla. Magn Reson Med 2010;63:1486–92.
[21] Weiger M, Wu M, Wurnig MC, Kenkel D, Boss A, Andreisek G, et al. ZTE imaging with long-T_2 suppression. NMR Biomed 2015;28:247–54.
[22] Weiger M, Pruessmann KP. MRI with zero echo time. Encyclopedia Magn Reson 2012;1:311–22.
[23] Weiger M, Wu M, Wurnig MC, Kenkel D, Jungraithmayr W, Boss A, et al. Rapid and robust pulmonary proton ZTE imaging in the mouse. NMR Biomed 2014;27:1129–34.